Synthetic AGB evolution II: the predicted abundances of PNe in the LMC

Groenewegen, M.A.T.; de Jong, T.

Link to publication

Synthetic AGB evolution

II. The predicted abundances of planetary nebulae in the LMC

M.A.T. Groenewegen[1] **and T. de Jong**[1,2]

[1] Astronomical Institute 'Anton Pannekoek', Kruislaan 403, NL-1098 SJ Amsterdam, The Netherlands
[2] SRON, Space Research Groningen, P.O. Box 800, NL-9700 AV Groningen, The Netherlands

Abstract. In Paper I of this series we presented a model to calculate in a synthetic way the evolution of AGB stars. The model was applied to the LMC and values were derived for the minimum core mass for third dredge-up, the dredge-up efficiency and the Reimers mass loss rate coefficient on the AGB. The observed carbon star luminosity function, the C/M-star ratio and the initial-final mass relation acted as constraints. In this paper we compare the predicted and observed abundances of planetary nebulae (PNe) in the LMC for the final model of Paper I. In general there is good agreement. The discrepancy between observations and predictions in the C/O-C/N diagram suggests that either the mass loss rate of the most massive stars is underestimated or that their is no dredge-up after hot-bottom burning ceases. From the N/O–N/H diagram we deduce that on the main sequence the ratio of the oxygen abundance to the total metallicity probably was higher in the past. This is consistent with observations of the oxygen abundance in the Galaxy as well as theoretical modelling of the chemical evolution for the LMC. The location of a PN in the N/O–He/H, C/O–He/H, C/O–C/N and N/O–N/H diagrams is a good indicator of the main-sequence mass. Our model predicts the high He/H and N/O ratios observed in some planetary nebulae.

Key words: stars: evolution of – planetary nebulae: general – Magellanic Clouds – stars: AGB, post – AGB

1. Introduction

Since planetary nebulae (PNe) have evolved from AGB stars one expects a relation between the abundances in the nebulae and in the photospheres of AGB stars. In this paper we compare the observed abundances of PNe in the LMC with the predictions of a synthetic AGB evolution

code. Preliminary results of this work were presented by Groenewegen & de Jong (1993).

We have developed a model to calculate the evolution of AGB stars in a synthetic way (Groenewegen & de Jong 1993a, Paper I). This model is more realistic than previous synthetic evolution models in that more details on the evolution have been included. The variation of the luminosity during the interpulse period is taken into account as well as the fact that, initially, the first few pulses are not yet at full amplitude and that the luminosity is lower than given by the standard core mass-luminosity relation. Most of the relations used are metallicity dependent.

The model uses algorithms derived from recent evolutionary calculations for low and intermediate mass stars. The main free parameters are the minimum core mass for (third) dredge-up M_c^{min}, the dredge-up efficiency λ and the Reimers mass loss coefficient on the AGB, η_{AGB}. By fitting the observed carbon star luminosity function (LF) in the LMC, the overall C/M-star ratio and the initial-final mass relation we showed in Paper I that the best model has $M_c^{min} = 0.58 M_\odot, \lambda = 0.75$, $\eta_{AGB} = 5$. We also showed that hot-bottom burning (HBB) on the level of Renzini & Voli's (1981; RV) $\alpha = 2$ case could well explain the observed number of high luminosity J-type carbon stars. This model will be referred to as the standard model. A brief description of the model is given in Sect. 2. Based on the standard model we compare the predicted abundances in the ejecta of model stars with the observed abundances of PNe in Sect. 3. After discussing the discrepancies between observations and predictions an improved model is presented in Sect. 4. We conclude in Sect. 5.

2. Theoretical AGB evolution

The model is described in full detail in Paper I. Some essential aspects, relevant to this paper, are briefly introduced here.

The observed population of AGB stars is modelled by randomly selecting stars from the distribution $N \, dM \sim$

IMF(M) SFR(M) $t_{AGB}(M) \, dM$ for $M_{lower} < M < M_{upper}$ where t_{AGB} is the lifetime on the AGB, IMF is the Initial Mass Function and SFR is the Star Formation Rate. The IMF-slope, SFR and age-metallicity relation for the LMC are adopted from van den Hoek & de Jong (1992). These relations were derived by simultaneously modeling the current gas fraction, current metallicity and age-metallicity relation for the LMC, constrained by the best available ages and metallicities of LMC clusters. Assuming a power-law IMF (IMF$\sim M^{-\alpha}$) and a density dependent SFR, the age-metallicity relation for the LMC was best modelled with $\alpha = -2.72$. The age of the LMC is taken as 11 Gyr, about equal to the age of the Galactic disk (Rocca-Volmerange & Schaeffer 1990). The pre-AGB lifetimes of Iben & Laughlin (1989) are used to relate the initial mass to the stellar lifetimes and initial metallicity. From this relation we find that stars down to $M_{lower} = 0.93 M_\odot$ have lived long enough to have reached the AGB. From Becker & Iben (1979) we derive an upper limit to the initial mass of AGB stars of $M_{upper} = 8.2 M_\odot$ for typical LMC abundances. A distance modulus to the LMC of 18.50 is adopted (Panagia et al. (1991).

Mass loss on the AGB is described by a Reimers (1975) law:

$$M = \eta_{AGB} 4.0 \, 10^{-13} \frac{LR}{M} \quad M_\odot/yr. \qquad (1)$$

The luminosity L is not the quiescent luminosity but includes the effect of the luminosity variation during the flash-cycle, so that the mass loss rate just after a TP is higher than during the H-burning phase or in the luminosity dip. In Paper I we found that $\eta_{AGB} \gtrsim 3$ is needed to fit the initial–final mass relation for the low mass stars and that $\eta_{AGB} = 5$ provides the best fit to the high-luminosity tail of the carbon star LF.

Tracks in the HR diagram are calculated using the $M_{bol} - T_{eff}$ relations of Wood (1990). The effects of first, second and third dredge-up are included. The algorithm to calculate the effects of the first dredge-up process is taken from RV but some of their numerical coefficients are updated using new results of Sweigart et al. (1989, 1990). The algorithm to calculate the effects of second dredge-up is taken from RV without change.

The third dredge-up process is described as follows. Dredge-up occurs only when the core mass is higher than a critical value M_c^{min}. In Paper I we found that $M_c^{min} = 0.58 M_\odot$ is needed to fit the low-luminosity tail of the carbon star LF. When there is dredge-up an amount of material

$$\Delta M_{dredge} = \lambda \, \Delta M_c \qquad (2)$$

is added to the envelope, where ΔM_c is the core mass growth during the preceding interpulse period. The composition of the dredged up material is assumed to be (Boothroyd & Sackmann 1988): $X_{12} = 0.22$ (Carbon), $X_{16} = 0.02$ (Oxygen) and $X_4 = 0.76$ (Helium). In Paper I we found that $\lambda = 0.75$ is needed to fit the peak of the carbon star LF. Hot bottom burning (HBB) has been included

at the level of the RV $\alpha = 2$ case (see Appendix A of Paper I).

3. The predicted abundances in PNe

In this section the observed abundances in LMC PNe are compared to the predicted abundances in the ejecta of our model stars for the standard model. The observed abundances are taken from Aller et al. (1987), Monk et al. (1988), Henry et al. (1989), Clegg (1991) and Dopita & Meatheringham (1991). The errors in the observed abundances are typically 0.015 in He/H and about 0.2 dex in all other ratios.

The abundances in the ejecta of the model stars are calculated by taking the average abundance in the material ejected during the final $5 \, 10^4$ yr on the AGB. This implies that a mean lifetime of the PN phase of $5 \, 10^4$ yr is assumed (Zijlstra & Pottasch 1991). The predicted abundances do not change significantly if a value of $2 \, 10^4$ yr is used for the mean lifetime of a PN.

We emphasize that we do not claim all our model stars to actually become PNe. We calculate the average abundances in the ejecta of the AGB star. Whether these ejecta will be recognised and classified as a PN is a different story. In fact, comparing the death rate of AGB stars and the birth rate of PNe in Paper I, one finds that a fairly large number of low mass stars will probably not become PNe or have so far not been identified as such.

We expect to find three distinct groups of stars. The first group consists of stars of $M_{initial} \lesssim 1.2 M_\odot$. These stars have core masses too low for the third dredge-up to occur. In these stars we expect to see the main-sequence abundances changed by the first dredge-up process only. The second group consists of stars in the initial mass range $1.2 M_\odot \lesssim M \lesssim 3.5 M_\odot$. After first dredge-up (and may be second dredge-up for the massive ones) these stars dredge-up carbon, helium and some oxygen on the AGB during thermal pulses (third dredge-up). We expect the C/O and He/H ratios to be enhanced. The third group consists of stars more massive than $M_{initial} \gtrsim 3.5 M_\odot$. In these stars, the carbon dredged-up during thermal pulses is largely converted to nitrogen by HBB. At the end of their life, when the envelope mass is below a critical value (M_{env}^{HBB}) and HBB is assumed to be no longer effective (see Appendix A of Paper I for details) unprocessed carbon is again added to the envelope.

In Fig. 1 observed and predicted abundance ratios are compared. The N/O–He/H diagram is a classical way to compare theoretical models with observations (see Clegg 1991 for references). The predictions of the RV models e.g. were not in agreement with the observations (see e.g. Kaler et al. 1990), in particular these models did not predict the high He/H and N/O ratios observed in some PNe. This has led to the suggestion that there was another mixing mechanism besides third dredge-up and HBB. Our model has no difficulty in predicting high He/H ratios. This is probably
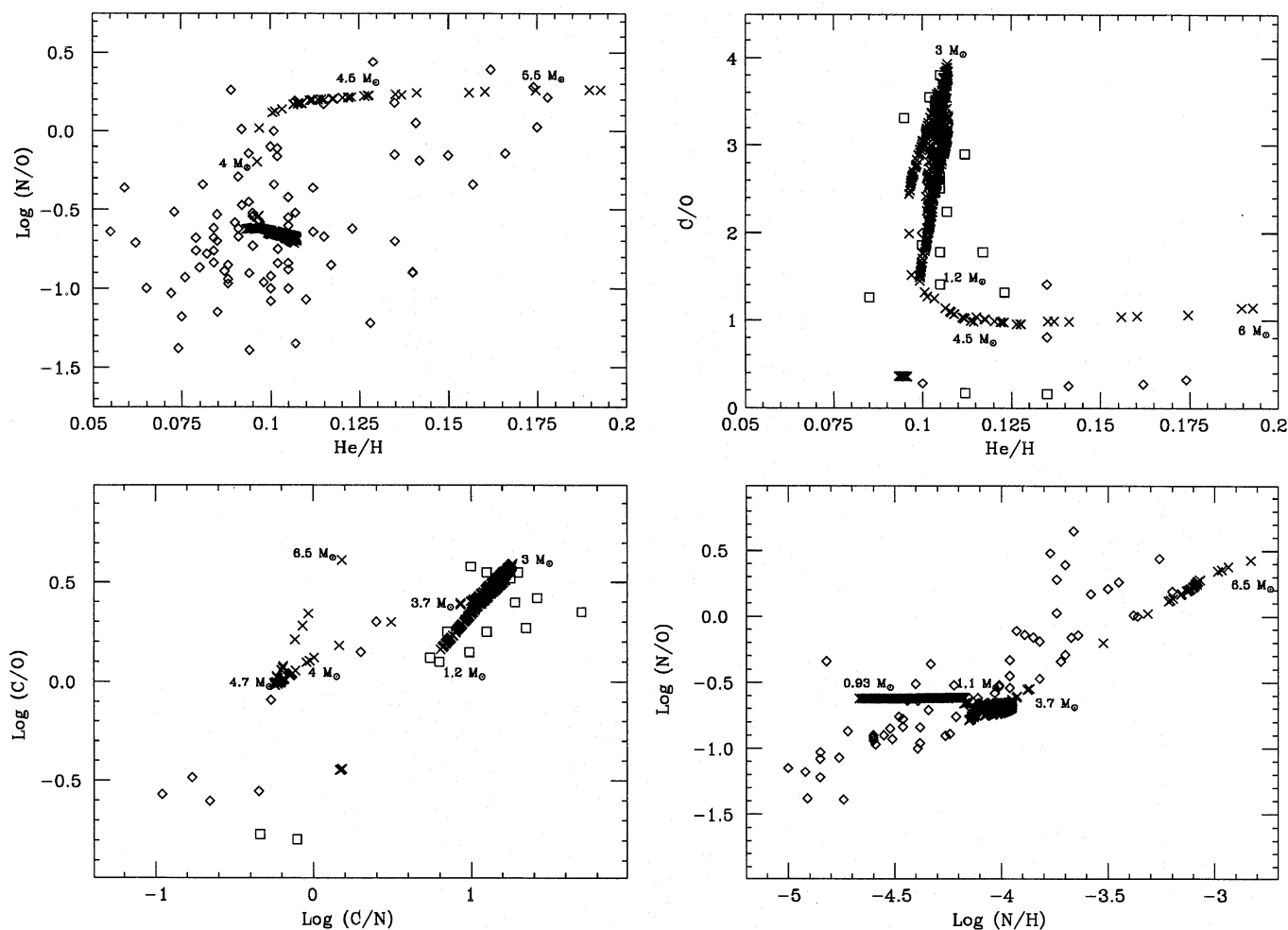
Fig. 1. Observed and predicted abundance ratios of planetary nebulae in the LMC for the standard model. Model results are plotted as crosses and some initial masses are indicated. In the C/O–He/H and C/O–C/N diagram the observed type I PNe (defined as having N/O > 0.5) are indicated by diamonds, the other observed PNe by squares. The density of points of the model stars with increasing initial mass reflects the initial mass function and the star formation rate history

due to the fact that RV ended the AGB evolution in their model with the sudden ejection of a PNe (of 0.5–$1.4 M_\odot$ depending on core mass). In our model AGB evolution ends when the envelope mass is typically $10^{-3} M_\odot$ (Sect. 2.7 of Paper I). Therefore, the stars in our model experience some additional thermal pulses and the effect of third dredge-up will be more pronounced. The type I PNe (defined as N/O > 0.5), resulting from HBB in our model, represent a sequence of increasing initial mass. The relation between N/O and core mass is discussed in Sect. 5.

The C/O–He/H panel in Fig. 1 shows a similar good agreement. The maximum C/O ratio observed is in good agreement with our prediction. This supports our combination of η_{AGB} and λ. If e.g. the mass loss rate would be much smaller, with λ fixed, the lifetime on the AGB would be prolonged, resulting in more thermal pulses and higher C/O ratios. Similarly, a higher value for λ, with fixed mass loss rate would also result in higher C/O ratios. Although combinations of higher η_{AGB} with lower λ or vice versa could

probably result in similar C/O ratios, other constraints (carbon star LF, C/M ratio) would not permit this (Paper I). The PNe which evolved from massive progenitors, the type I PNe (indicated by diamonds), are located at high He/H ratios. Note that they have C/O ratios between 0.8 and 1.2, while the observations indicate lower ratios.

The segregation of stars of different initial masses is most clearly demonstrated in the C/O–C/N diagram. The C/O ratio traces the third dredge-up process, while the C/N ratio is sensitive to the CNO-cycle. The observed type I PNe are indicated by diamonds, the other PNe by squares. The low mass (model) stars are all located near C/N ≈ 1.5, C/O ≈ 0.35, the abundance ratios after the first dredge-up. Their observed counterparts are the two PNe near C/N ≈ 0.6, C/O ≈ 0.16. It is unclear if this discrepancy is real. An uncertainty is that the carbon abundance is difficult to determine and different methods do not agree (see e.g. Clegg 1991). Clearly, reliable carbon abundances must be determined for more (low-luminosity) PNe.

The intermediate mass stars are located at C/O > 1.0, C/N > 5. The observation and predictions agree perfectly. The massive stars experiencing HBB represent a sequence which neatly follows the observations up to $\sim 4.7 M_\odot$, but then, apparently, carbon is added and the sequence turns upwards and to the right. This is in contradiction with the observations which suggest that the C–N conversion is more active resulting in the PNe located at C/O $\approx$ 0.25, C/N $\approx$ 0.20.

The reason why carbon is added to the envelope of the most massive stars in our model at the end of their life is as follows. HBB is assumed to be effective until the envelope mass is below a critical value (M_{env}^{HBB}). This mimics the fact that only when the envelope is massive enough the high temperatures needed for HBB can be sustained. In our model, when HBB ceases, the third dredge-up process continues to be effective and adds carbon to the envelope. In Paper I, M_{env}^{HBB} was determined by fitting our model to the models of RV. We found that M_{env}^{HBB} is in the range 0.4–0.8$M_\odot$ for stars with core masses between 0.8 and 1.0 $M_\odot$. The most massive stars ($\gtrsim 4.7 M_\odot$) live long enough to experience thermal pulses which add carbon to the envelope, between the time that the envelope mass becomes less than M_{env}^{HBB} and the end of the AGB. This is not true for the less massive stars (3.5–4.7$M_\odot$) due to the fact that M_{env}^{HBB} decreases (i.e. shorter lifetimes) with decreasing core mass (i.e. lower initial mass) and that the interpulse period increases with decreasing core mass. The comparison of the predicted and observed abundances of the massive stars suggest that the following (combination) of effects could be playing a role: (1) M_{env}^{HBB} is lower than assumed, (2) there is no dredge-up after HBB ceased ($\lambda = 0$), (3) the interpulse period has been underestimated for the massive stars, (4) mass loss has been underestimated for the massive stars. We do not favor the last two explanations since they imply selective effects only applying to the massive stars. There are no other indications that the interpulse period or the mass loss rate have been underestimated. In fact, in Paper I we showed that a mass loss rate higher than $\eta_{AGB} = 5$ is in disagreement with the high-luminosity tail of the carbon stars LF, and predicts a C/M ratio which is lower than observed. In Sect. 4 we show that a model with $\lambda = 0$ after HBB ceases reproduces the observations well.

In the N/O–N/H diagram we see that the observations indicate a tight correlation between N/O and N/H. Our results confirm this relation for stars more massive than $\sim 1.1 M_\odot$. For stars of lower mass a decreasing mass results in lower N/H (because Z is lower), but N/O remains constant, because of the original model assumption that the main sequence abundances of C, N and O relative to the total metallicity have solar values and the fact that the effects of the first dredge-up are not very mass dependent. The comparison of observations and predictions suggest that the relative main-sequence abundances of C, N and O change with Z and/or the effects of first dredge-up are mass dependent. These effects seem only to play a role below $\sim 1.1 M_\odot$

and therefore do not effect the conclusions of Paper I about the formation and evolution of carbon stars in the LMC, which occurs around or above $\sim 1.2 M_\odot$.

Can we distinguish between variations in the main sequence abundances and a mass dependent first dredge-up process? The observations indicate that for lower Z, N/O should be smaller. A lower nitrogen abundance seems unlikely since this would increase the discrepancy for the low mass stars in the C/O–C/N diagram. A higher oxygen abundance would make this discrepancy smaller. This suggests main sequence rather than first dredge-up variations, since oxygen is hardly converted into nitrogen during the first dredge-up.

In the Galaxy the relative amount of oxygen has been higher in the past (Wheeler et al. 1989). This is due to the fact that oxygen is mainly produced in massive stars. Based on the abundances of the PNe we conclude that a similar history of the oxygen abundance applies to the LMC. Recently, Russell & Dopita (1992) by modelling the chemical evolution of the LMC showed that [O/Fe] was indeed higher in the past.

4. The final model

Based on the results of Paper I and the discussion in the previous section our final model for the LMC has the following parameters: $M_c^{min} = 0.58 M_\odot$, $\lambda = 0.75$, $\eta_{AGB} = 5.0$, as before. HBB is still included but we now assume no dredge-up after HBB ceases. In addition the relative main-sequence oxygen abundance is given by $(O/Z) = 1/(1 + 0.838(Z/Z_0)^{0.7})$, where Z_0 is the present-day metallicity in the LMC. The exponent in this empirical relation was determined by fitting the observations for log(N/H) < −4.2 in the N/O–N/H diagram. The present-day (O/Z) ratio is $1/(1 + 0.838) = 0.544$, the ratio assumed in Paper I (Sect. 2.9.1).

The predicted and observed abundances of PNe are shown in Fig. 2 for the final model. In the N/O–He/H diagram the main change with respect to Fig. 1 is the N/O ratio of the low mass stars. Stars of $\sim 0.9 M_\odot$ are located at log(N/O) $\approx$ −1.1, stars of $1.2 M_\odot$ at log(N/O) $\approx$ −0.7. In the C/O–He/H diagram the main change is in the C/O ratio of the massive stars due to the enhanced oxygen abundance. The C/O ratios are now ~ 0.5, in much better agreement with observations. In the C/O–C/N diagram the changes are twofold. The C/O ratio of the low mass stars is lower and because dredge-up is assumed to stop when HBB ceases, the PNe of massive progenitors now evolve to log(C/O) $\approx$ −0.3, log(C/N) $\approx$ −0.8, in reasonable agreement with observations. The assumption that $\lambda = 0$ after HBB stops is rather ad-hoc. Lattanzio (1989) has found cases (for low mass stars) where λ is 0 at some thermal pulses. That this process also occurs for massive stars after the end of HBB has yet to be demonstrated. An alternative hypothesis is that the mass loss rate of the most massive stars is underestimated. With a Reimers law, the
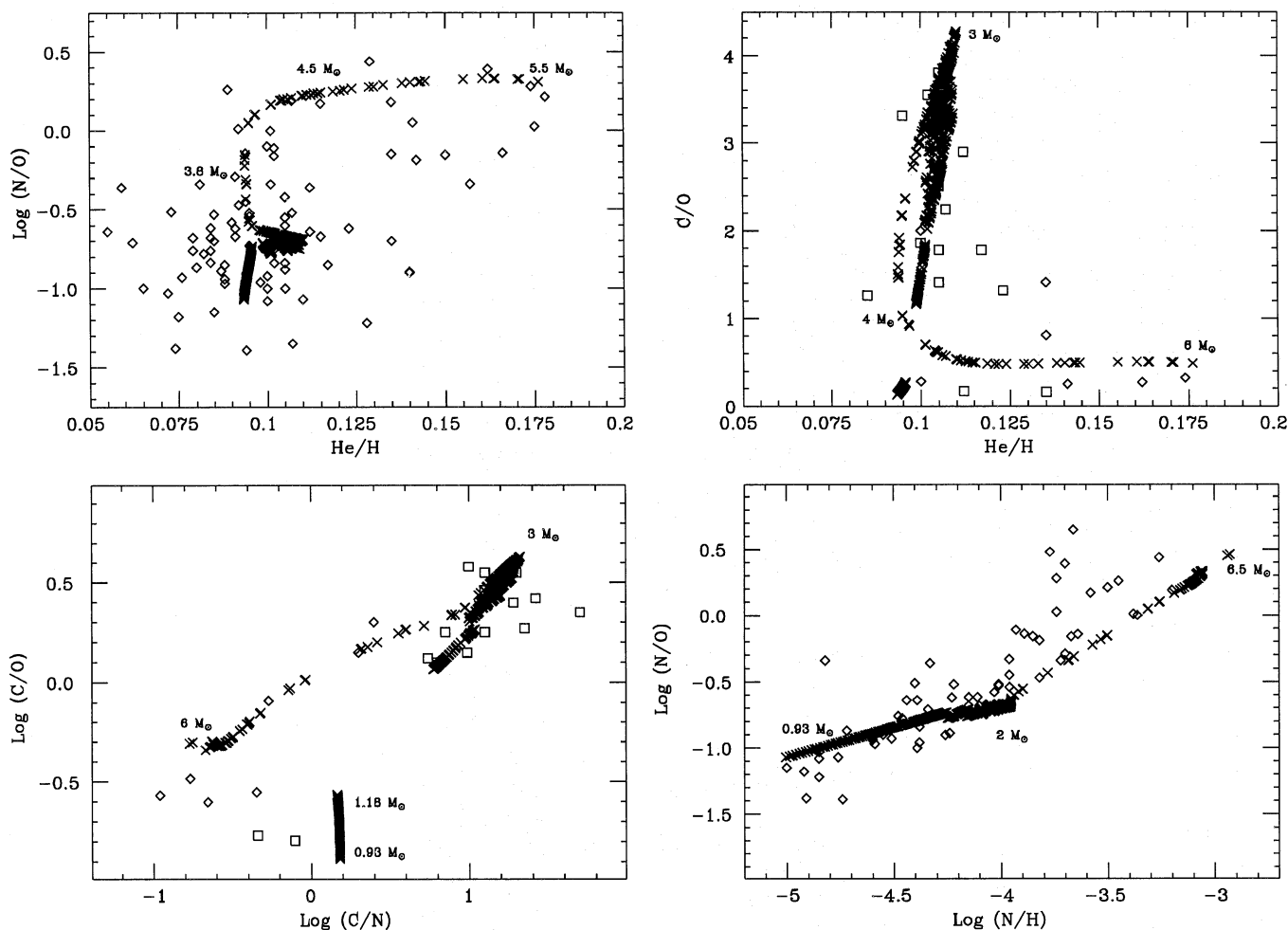
Fig. 2. Observed and predicted abundance ratios of planetary nebulae for the final model. Model results are plotted as crosses and some initial masses are indicated. In the C/O–He/H and C/O–C/N diagram the observed type I PNe are indicated by diamonds, the other observed PNe by squares

mass loss rates of the massive stars cannot be increased without violating the constraints used in Paper I (C/M star ratio, C-star luminosity function). In a future publication (Groenewegen & de Jong 1993b) we investigate the influence of different mass loss rate laws (proposed by Vassiliadis & Wood 1993 and Blöcker & Schönberner 1992) and show that with a mass loss rate law with a steeper luminosity dependence than Reimers law the assumption $\lambda = 0$ after HBB stops is not necessary. In the N/O–N/H diagram the main change is in the N/O ratio for the low mass stars. With our adopted variation of the main-sequence oxygen abundance, the N/O–N/H diagram can be explained well for the low mass stars.

The scatter of the observations around the model predictions in Fig. 2 is probably due to both observational uncertainties and uncertainties in the model assumptions. The former were already discussed and amount to about 0.015 in He/H and about 0.2 dex in the other abundance ratios. For the low mass stars ($M \lesssim 1.2 M_\odot$), which do not experience the third dredge-up, the predicted abundances are determined by the main sequence abundances and the first

dredge-up process. We assumed an uniform age-metallicity relation and relative solar abundances for the CNO elements on the main sequence (except in Fig. 2, where the relative oxygen abundance is a function of metallicity). These two assumptions will probably not reflect the true chemical evolution history of different parts of the LMC for the different elements.

The largest uncertainty for the high mass stars ($M \gtrsim 3.5 M_\odot$) is probably the parameterization of HBB in our model. The RV $\alpha = 2$ case used in our model provides a good fit to the high-luminosity J-type carbon stars (Paper I) and the PNe abundances of the massive stars. However, we are unable to explicitly test how e.g. the RV $\alpha = 1.5$ case would fit the observations since RV did not present the necessary data regarding the temperatures at the bottom of the convective envelope.

5. Discussion

Since PNe evolve from AGB stars it would be interesting to compare their abundances. Unfortunately, there are

no CNO abundance determinations available for AGB stars in the LMC. For the galaxy they have been compared by Smith & Lambert (1990). They note that while the C/O ratio in (disk-) PNe ranges up to about 4, the maximum C/O ratio in carbon stars is only about 1.4 (Lambert et al. 1986). Smith & Lambert suggest systematic errors, the obscuration of more carbon-rich stars by dust and the possibility that C-rich PNe receive their enrichment just before the superwind strips the AGB star of its envelope, as possible explanations. Dust obscuration seems not very likely. In Paper I we showed, based on the observed number of IRAS sources in the LMC, that dust obscuration cannot be very important. For the galaxy, Groenewegen & de Jong (1993c) showed that in a sample of fourteen infrared carbon stars, eight in fact have optical counterparts.

From a theoretical point of view there is a clear relation between N/O and final core mass as shown by Becker & Iben (1980) and RV. In Fig. 3 the N/O–M_c-relation is plotted for our LMC model. The N/O ratio is almost flat up to $M_c = 0.84 M_\odot$, then steeply rises and finally levels of around N/O ≈ 2. The curve up to the steep rise is determined by the initial abundances and the changes during first, second and third dredge-up. The location of the steep rise and the high core mass curve are determined by HBB. From an observational point of view the hypothesis that type I PNe originate from massive progenitors has been tested by constructing a N/O versus core mass diagram (Kaler et al. 1990; Kaler & Jacoby 1990; Stasińska & Tylenda 1990). The N/O ratio is determined from an abundance analysis while the core mass of the PNe is inferred by plotting the star in a HR diagram and the position compared to the tracks of post-AGB stars, or a core mass-luminosity relation is used. Excluding some uncertain points Kaler et al. (1990) claim there is "a strong and convincing" relation between N/O and M_c. The same conclusion is reached by Stasińska & Tylenda (1990). Ratag (1991) and Pottasch (1992) however, state there is no observa-

tional evidence for such a relation. Ratag (1991) criticize Kaler et al. and Stasińska & Tylenda for making use of the Shklovskii method to derive distances which enter the luminosity determination. However, Kaler & Jacoby (1990) also find a relation between N/O and M_c for PNe in the LMC and SMC. Furthermore, the sudden increase in N/O at $M_c \approx 0.8 M_\odot$ due to HBB is not expected in the sample of galactic bulge PNe studied by Ratag. Galactic bulge PNe (GBPNe) are thought to have evolved from stars of initial mass $< 1.3 M_\odot$ (Ratag 1991). The core masses of GBPNe have been determined using different core mass-luminosity relations and different methods and are found to be $< 0.68 M_\odot$ (Ratag 1991; Tylenda et al. 1991). For such low core masses HBB is probably not important and the scatter in the N/O vs. core mass diagram is expected to be entirely due to initial abundance variations and the effect of first and third dredge-up.

There are several problems in determining the core mass of a PN from its position in the HR diagram. Firstly, the uncertain distances to galactic PNe enter the luminosity determination. Secondly, a non-negligible amount of PNe may have evolved from He shell-burning AGB stars. From theory it is expected that $\sim 30\%$ of stars are He-burners when they leave the AGB (the duration of the luminosity dip relative to the interpulse period). Of the 22 AGB models recently calculated by Vassiliadis & Wood (1993), 6 left the AGB when burning helium (= 27%). Since usually post-AGB tracks or core mass-luminosity relations for quiescent H shell-burning are used to determine the core mass, this underestimates M_c by $\sim 0.05 M_\odot$ for low core masses and by $\sim 0.1 M_\odot$ for stars with $M_c \approx 0.7 M_\odot$ in 30% of the cases. Because it is exceedingly difficult to determine observationally if a PN has evolved from a H or a He shell-burning AGB star, this uncertainty may inhibit a detailed observational study into the role of HBB (and the distribution of the masses of PNe for that matter) even when the distances to PNe are known accurately.
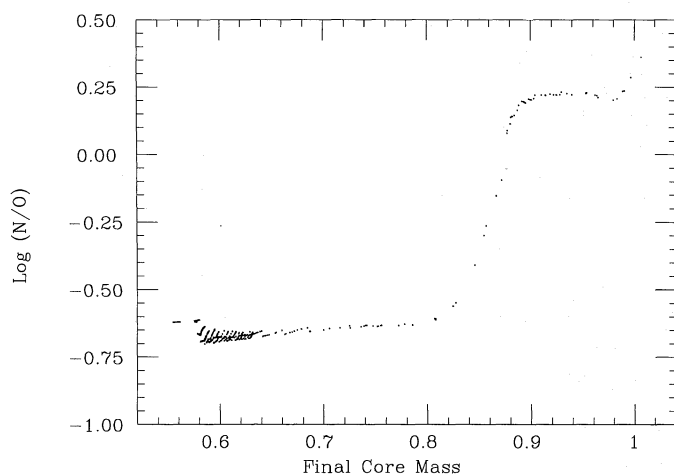
Fig. 3. The theoretical relation between N/O in PNe and the final core mass on the AGB for the LMC model stars

References

Aller L.H., et al., 1987, ApJ 320, 159
Becker S.A., Iben I., 1979, ApJ 232, 831
Becker S.A., Iben I., 1980, ApJ 237, 111
Blöcker T., Schönberner D., 1992, in: Weinberger R., Acker A. (eds.) Proc. IAU symp. 155 on Planetary Nebulae, Reidel, Dordrecht (in press)
Boothroyd A.I., Sackmann I.-J., 1988, ApJ 328, 653
Clegg R.E.S., 1991, in: Michaud G., (eds.) Tutukov A., Evolution of stars, Proc. IAU symp. 145, Reidel, Dordrecht, p. 387
Dopita M.A., Meatheringham S.J., 1991, ApJ 377, 480

Groenewegen M.A.T., de Jong T., 1993, in: Weinberger R., Acker A. (eds.) Proc. IAU symp. 155 on Planetary Nebulae, Reidel, Dordrecht (in press)

Groenewegen M.A.T., de Jong T., 1993a, A&A 267, 410 (Paper I)

Groenewegen M.A.T., de Jong T., 1993b, A&A (in press)

Groenewegen M.A.T., de Jong T., 1993c, A&AS (in press)

Henry R.B.C., Liebert J., Boroson T.A., 1989, ApJ 339, 872

Iben I., Laughlin G., 1989, ApJ 341, 312

Kaler J.B., Jacoby G.H., 1990, ApJ 362, 491

Kaler J.B., Shaw R.A., Kwitter K.B., 1990, ApJ 359, 392

Lambert D.L., Gustafsson B., Eriksson K., Hinkle K., 1986, ApJS 62, 373

Lattanzio J.C., 1989, ApJ 344, L25

Monk D.J., Barlow M.J., Clegg R.E.S., 1988, MNRAS 234, 583

Panagia N., Gilmozzi R., Macchetto F., Adorf H.-M., Kirshner R.P., 1991, ApJ 380, L23

Pottasch S.R., 1992, in: Weinberger R., Acker A. (eds.) Proc. IAU symp. 155 on Planetary Nebulae, Reidel, Dordrecht (in press)

Ratag M.A., 1991, Ph.D. Thesis, Chap. 5, University of Groningen

Reimers D., 1975, in: Basheck B., et al. (eds.) Problems in stellar atmospheres and envelopes. Springer, Berlin, p. 229

Renzini A., Voli M., 1981, A&A 94, 175 (RV)

Rocca-Volmerange B., Schaeffer R., 1990, A&A 233, 427

Russell S.C., Dopita M.A., 1992, ApJ 384, 508

Smith V.V., Lambert D.L., 1990, ApJS 72, 387

Stasińska G., Tylenda R., 1990, A&A 240, 467

Sweigart A.V., Greggio L., Renzini A., 1989, ApJS 69, 911

Sweigart A.V., Greggio L., Renzini A., 1990, ApJ 364, 527

Tylenda R., Stasińska G., Acker A., Stenholm B., 1991, A&A 246, 221

Van den Hoek L.B., de Jong T., 1992, in preparation

Vassiliadis E., Wood P.R., 1993, ApJ 413, 641

Wheeler J.C., Sneden W., Truran J.W., 1989, ARA&A 27, 279

Wood P.R., 1990, in: Mennessier M.O., Omont A. (eds.) From miras to planetary Nebulae, Editions Frontieres, Gif-sur-Yvette, p. 67

Zijlstra A.A., Pottasch S.R., 1991, A&A 243, 478